

INVESTIGATIONS ON THE PHENOMENON OF HYSTERESIS IN SINGLE-PHASE NATURAL CIRCULATION LOOPS

Naveen Kumar¹, J. B. Doshi² and P. K. Vijayan¹

¹Reactor Engineering Division

Bhabha Atomic Research Centre, Trombay, Mumbai - 400085, India

²Department of Mechanical Engineering

Indian Institute of Technology, Powai, Mumbai - 400076, India

Email of corresponding author: knaveen@barc.gov.in

ABSTRACT

In this paper, a model is proposed for simulating the expansion tank used in single-phase natural circulation experimental facilities. The proposed model is integrated with a 1-D model developed previously by the authors. Numerical simulations bring out the role of expansion tank in loop dynamics. The physics of hysteresis has been brought out. The paper compares the model predictions with observed experimental behaviour.

INTRODUCTION

Natural circulation phenomenon play an important role in transporting energy from hot zones to cold zones without using a mechanical pump in several engineering systems, such as nuclear power plants, solar energy heating and cooling systems, geothermal systems, electrical machine rotor cooling, turbine blade cooling and electronic device cooling. The principal characteristics of the natural circulation systems is that liquid circulation is achieved by buoyancy force, which is the result of thermally induced density differences in the liquid in the presence of a body force like gravitational force, centrifugal force and coriolis force. Since these systems do not require any moving parts (pump) for their operation, they find extensive applications in nuclear industry for core heat removal. This is because of their high reliability and relatively low maintenance cost.

Over the decades considerable research efforts have been spent to analyze the steady state and dynamic behavior of natural circulation loops. They have been subjected to extensive numerical and experimental investigations. The experimental observations show that these loops can exhibit different oscillatory modes depending upon the operating conditions. Stability and transient analysis of single-phase natural circulation loops have been carried out using both sophisticated system codes like ATHLET [1], RELAP [2-4] and CATHARE [2]; and simple tools [5-16]. However, numerical simulations of the observed behavior have been only partially successful. Vijayan et al. [10] carried out experimental investigations in rectangular single-phase natural circulation loops having different heater and cooler orientations. In these investigations, instability was observed only with horizontal orientation for both the heater and the cooler. Further, the stable regime was found to be dependent on heat addition path. During power raising from stable steady state, the threshold power for instability was found to be 270 W and only bidirectional pulsing flow behaviour was observed. However, during power step back experiments, the stable steady flow behaviour was observed only at power below 65 W. The existence of conditionally stable regimes was termed as hysteresis by the authors. None of the numerical tools have been successful in simulating the following observed behavior [10] in single-phase natural circulation loops having horizontal heater and horizontal cooler:

- the startup from rest, and
- the phenomenon of hysteresis.

The theoretical models available in literature are too simple to take into account the complex behaviour exhibited by these loops. The inadequacy of 1-D models in predicting the observed system behaviour is not difficult to comprehend. Most of the 1-D models, including the systems codes used for safety analysis of nuclear reactor systems, are based on several simplifying assumptions, whose adequacy in predicting the behaviour of single-phase natural circulation systems is highly questionable. These are summarized below:

- the neglect of natural convection and mixed convection regimes;
- the neglect of axial heat conduction along the heated walls and in the bulk fluid;

- the use of constitutive laws for friction and heat transfer derived from steady state forced convection experiments;
- the neglect of developing boundary layer conditions in heated and cooled sections;
- the lack of proper numerical model for expansion tank;
- the use of first order numerical schemes;
- the use of 1-D balance equation based on cross-section averaged variables.

The validity of first two assumptions was investigated by Naveen Kumar et al. [16]. It was observed that it is not possible to simulate the start-up from rest state without considering the natural convection and mixed convection. They developed a semi-empirical model for natural convection and mixed convection and successfully incorporated the same in a 1-D model developed by them. They successfully simulated the start-up from rest of natural circulation loops having horizontal heater and horizontal cooler. The different dynamic flow characteristics like unidirectional pulsation, bidirectional pulsation and chaotic pulsations were also simulated. However, predictions made using wall constitutive laws developed for friction and heat transfer from steady forced convection experiments could not simulate the existence of lower stability threshold.

In this paper, a model is developed for expansion tank, installed in single-phase natural circulation loops to accommodate the swell and shrinkages. The proposed model brings out physics of phenomenon of hysteresis observed by Vijayan et al. [11].

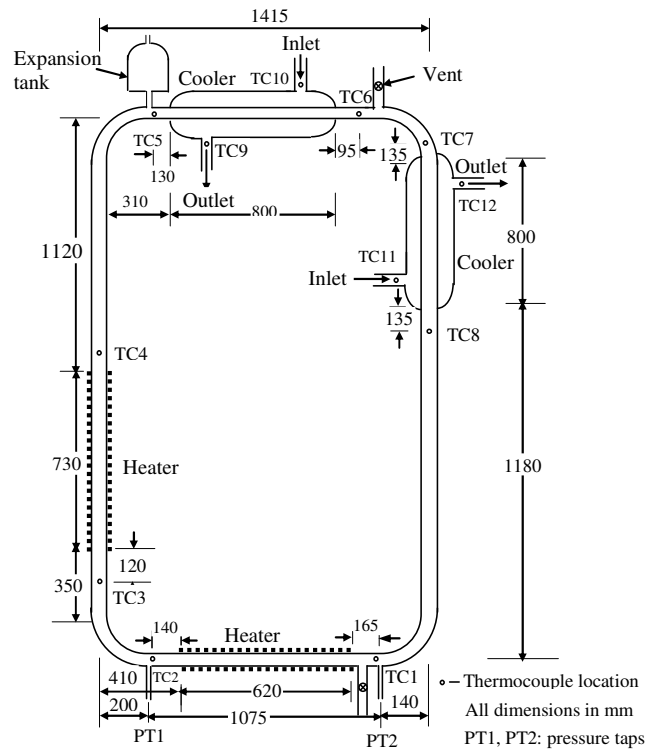


Fig. 1: Schematic of experimental loop [11]

OVERVIEW OF EXPERIMENTS

Experimental Loop

The addressed experimental loop consists of a uniform diameter rectangular natural circulation loop. The details of the experimental setup are given in Vijayan et al. [10]. It is made up of borosilicate glass tubes of inside diameter 26.9mm and outside diameter 28.9mm. Test loop has two heaters and two coolers. The lengths of the vertical and horizontal heaters are 620mm and 735mm respectively. One of the coolers is placed in the horizontal section at the uppermost elevation and the other cooler is placed in vertical pipe section. The dimensions of various

sections are as shown in Fig. 1. Each cooler is 800 mm long and having outside diameter 49.2 mm with 1.5 mm wall thickness. The coolant flow to the secondary side of the cooler is provided from an overhead tank. The loop also has an expansion tank located at the highest elevation to take care of swell and shrinkages in the loop fluid. The expansion tank, located at the highest elevation is connected to the loop by a 21 mm ID and 24 mm OD tube. To minimize the heat loss to atmosphere, the loop was insulated with ceramic wool. Twelve mineral insulated 0.5 mm diameter K-type thermocouples with measurement accuracy of 0.4% (of the span) were used to measure the pipe centreline temperatures at different locations shown in Fig 1. Pressure difference across a 1075 mm long section of the bottom horizontal tube was measured with the help of a calibrated differential pressure transmitter, with a measuring accuracy of 0.25% of span. The range of the differential pressure transmitter was -100 Pa to + 100 Pa. The coolant flow rate to cooler was maintained at 5l/min during all the tests. The coolant temperature was 30 °C. The heater was made up of 1 mm diameter nichrome wire evenly wound on the outside of the glass tube. The heater power was varied with the help of a dimmerstat and was measured using a wattmeter, which had an accuracy of 0.5% of the span (0-1250W). During the transient and stability experiments, the digital data were acquired on floppy disk.

Main Results for Horizontal Heater and Horizontal Cooler Configuration

It is possible to operate the experimental facility with different heater and cooler combinations. The one addressed in the present study is Horizontal Heater and Horizontal Cooler (HHHC) configuration. This is because of the reason that instability and hysteresis has been observed only with this configuration. The rest of the configurations have been found to be showing stable behaviour without any hysteresis effect. In the HHHC configuration, the following flow regimes were observed by Vijayan et al. [10, 11]:

- (a) For start up from rest, steady unidirectional flow was observed at heater power inputs below 102 W.
- (b) For start up from rest, unidirectional pulsing flow instability was observed for heater power inputs, $102 \text{ W} < Q < 135 \text{ W}$.
- (c) For start up from rest, bidirectional pulsing flow instability was observed for heater power inputs, $196 \text{ W} < Q < 408 \text{ W}$.
- (d) During start up from rest, switching between unidirectional and bidirectional pulsing flow was observed for heater power inputs, $135 \text{ W} < Q < 196 \text{ W}$.
- (e) For start-up from rest, compound instability was observed for heater power inputs greater than 408 W.
- (f) During power raising from stable steady state, the threshold of instability shifted from 102 W to 270 W and only bidirectional pulsing flow behaviour was observed.
- (g) During power step back experiments, the stable steady flow behaviour was observed only at power below 65 W.

MATHEMATICAL MODEL

Governing equations

The mathematical model is based on the following simplifying assumptions:

- (a) the flow can be represented by a 1-D description that does not take into account for radial variation of the fluid properties;
- (b) heat generation in the fluid due to frictional dissipation is neglected;
- (c) the kinetic energy term in the energy balance equation. is neglected;
- (d) each fluid element is in thermal contact with a heat structure and a convective heat transfer boundary condition can be assigned to the outside surface of the structure, specifying the outer fluid temperature and the outer heat transfer coefficient; and
- (e) for a nearly incompressible fluid natural convection consists of two equal and opposite streams moving between cold and warm sections. There is zero net mass transfer between the two sections and a net energy exchange. The energy change can be accounted in the area averaged energy balance equation.

With the above assumptions the governing mass, momentum and energy balance equations for flow through a channel can be written as:

Mass conservation equation

$$\frac{\partial \rho}{\partial t} + \frac{1}{A} \frac{\partial W}{\partial s} = 0 \quad (1)$$

Momentum conservation equation

$$\frac{1}{A} \frac{\partial W}{\partial t} + \frac{1}{A} \frac{\partial}{\partial s} \left(\frac{W^2}{\rho A} \right) = -\frac{f}{D_h} \frac{W^2}{2\rho_1 A^2} - \frac{\partial p}{\partial s} - \rho g \sin \theta \quad (2)$$

Energy conservation equation

$$\frac{\partial}{\partial t} (\rho h) + \frac{1}{A} \frac{\partial}{\partial s} (Wh) - \frac{\partial p}{\partial t} = \frac{h_i P (T_w - T_f)}{A} + \frac{1}{A} \frac{\partial}{\partial s} \left(AK_f \frac{\partial T}{\partial s} \right) \quad (3)$$

Equation of state

$$\rho = \rho(p, h) \quad (4)$$

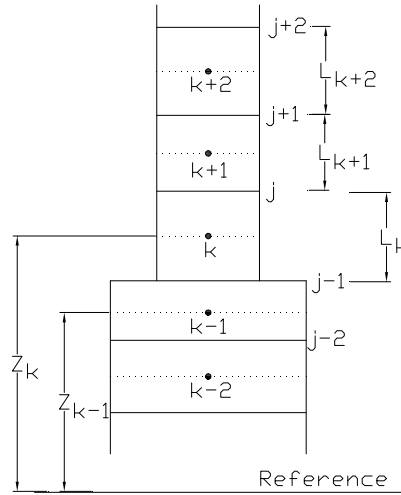


Fig. 2: Mesh cell labeling convention

Discretized equations

For the solution of governing equations by numerical technique, staggered mesh approach is used. The computational domain is divided into non overlapping rigid control volumes, called cells. The field variables, h , p and ρ are defined at the cell centers, while the fluid mass velocity, W is defined at cell interfaces also called junctions. The mesh cell configuration and labeling conventions for cell edges and cell centers are depicted in Fig. 2. The mass and energy equations are discretized by integrating over the mesh cells indicated by solid lines and the momentum balance equation. is discretized and integrated over the dashed mess cells. The resulting difference equations are:

Mass conservation equation.

$$\rho_k^{n+1} = \rho_k^n - \frac{1}{A_k} \frac{(W_j^{n+1} - W_{j-1}^{n+1})}{l_k} \Delta t \quad (5)$$

Momentum conservation equation

$$-p_k^{n+1} \Delta t + (I_j + C_j) W_j^{n+1} + p_{k+1}^{n+1} \Delta t = O_j^n \quad (6)$$

where

$$C_j^n = - \left[\left(\frac{f}{D_h A^2} \frac{l}{4\rho} \right)_k^n + \left(\frac{f}{D_h A^2} \frac{l}{4\rho} \right)_{k+1}^n \right] (|W|)_j^n \Delta t \quad (7)$$

$$I_j = \frac{l_k}{2A_k} + \frac{l_{k+1}}{2A_{k+1}} \quad (8)$$

$$O_j^n = I_j W_j^n - \left[\left(\frac{W^2}{\rho A^2} \right)_{k+1}^n - \left(\frac{W^2}{\rho A^2} \right)_k^n \right] \Delta t - \left(\frac{W^2}{2\rho} \right)_j^n \left[\frac{1}{A_{k+1}^2} - \frac{1}{A_k^2} \right] \Delta t - \left\{ \rho_{k+1}^n (z_{k+1} - z_j) + \rho_k^n (z_j - z_k) \right\} g \Delta t \quad (9)$$

Energy conservation equation

From Eq. (4), density can be expressed as

$$\frac{\partial \rho}{\partial t} = \frac{\partial \rho}{\partial h} \Big|_p \frac{\partial h}{\partial t} + \frac{\partial \rho}{\partial p} \Big|_h \frac{\partial p}{\partial t}$$

Using Eq. (1), the above equation is written as

$$\frac{\partial \rho}{\partial h} \Big|_p \frac{\partial h}{\partial t} + \frac{\partial \rho}{\partial p} \Big|_h \frac{\partial p}{\partial t} + \frac{1}{A} \frac{\partial W}{\partial s} = 0 \quad (10)$$

The energy conservation Eq. (3) is written in the following non conservative form

$$h \frac{\partial \rho}{\partial t} + \rho \frac{\partial h}{\partial t} + \frac{1}{A} \frac{\partial}{\partial s} (Wh) - \frac{\partial p}{\partial t} = \frac{h_i P (T_w - T_f)}{A} + \frac{1}{A} \frac{\partial}{\partial s} \left(AK_f \frac{\partial T}{\partial s} \right) \quad (11)$$

Using Eq. (1), Eq. (11) is written as

$$-\frac{h}{A} \frac{\partial W}{\partial s} + \rho \frac{\partial h}{\partial t} + \frac{1}{A} \frac{\partial}{\partial s} (Wh) - \frac{\partial p}{\partial t} = \frac{h_i P (T_w - T_f)}{A} + \frac{1}{A} \frac{\partial}{\partial s} \left(AK_f \frac{\partial T}{\partial s} \right) \quad (12)$$

Integration of Eq. (12) over control volume 'k' gives

$$\begin{aligned} & \rho_{|k}^n \frac{h_k^{n+1} - h_k^n}{\Delta t} + \frac{1}{A_k} \frac{W_j^{n+1} h_j^n - W_{j-1}^{n+1} h_{j-1}^n}{l_k} - \frac{h_k^n}{A_k} \left(\frac{W_j^{n+1} - W_{j-1}^{n+1}}{l_k} \right) - \frac{(p_k^{n+1} - p_k^n)}{\Delta t} = \\ & \frac{h_{i,k} P_k (T_w^{n+1} - T_f^n)}{A_k} + \frac{1}{A_k l_k} \left[A_j \left(\frac{T_{k+1}^n - T_k^n}{\left(\frac{l_{k+1}}{(K_f)_{k+1}} + \frac{l_k}{(K_f)_k} \right)} \right) - A_{j-1} \left(\frac{T_k^n - T_{k-1}^n}{\left(\frac{l_k}{(K_f)_k} + \frac{l_{k-1}}{(K_f)_{k-1}} \right)} \right) \right] \end{aligned} \quad (13)$$

Integration of Eq. (10) over the control volume 'k' gives

$$\frac{\partial \rho}{\partial h} \Big|_{p,k}^n (h_k^{n+1} - h_k^n) l_k + \frac{\partial \rho}{\partial p} \Big|_{h,k}^n (p_k^{n+1} - p_k^n) l_k + \frac{1}{A_k} (W_j^{n+1} - W_{j-1}^{n+1}) \Delta t = 0 \quad (14)$$

Substitution for $(h_k^{n+1} - h_k^n)$ from Eq. (14) into Eq. (13) and rearranging gives

$$\Gamma_{j,k}^n W_j^{n+1} = \Gamma_{j-1,k}^n W_{j-1}^{n+1} + \Omega_k^n p_k^{n+1} + \Theta_k^n \quad (15)$$

where

$$\Gamma_{j,k}^n = \frac{\partial \rho}{\partial h} \Big|_{p,k}^n (h_j^n - h_k^n) - \rho_{|k}^n \quad (16)$$

$$\Gamma_{j-1,k}^n = \frac{\partial \rho}{\partial h} \Big|_{p,k}^n (h_{j-1}^n - h_k^n) - \rho \Big|_k^n \quad (17)$$

$$\Omega_k^n = \frac{A_k l_k}{\Delta t} \left(\frac{\partial \rho}{\partial h} \Big|_{p,k}^n + \rho \Big|_k^n \frac{\partial \rho}{\partial p} \Big|_{h,k}^n \right) \quad (18)$$

$$\Theta_k^n = \frac{\partial \rho}{\partial h} \Big|_{p,k}^n h_{i,k} P_k (T_w^{n+1} - T_f^n) - \frac{A_k l_k}{\Delta t} \left(\frac{\partial \rho}{\partial h} \Big|_{p,k}^n + \rho \Big|_k^n \frac{\partial \rho}{\partial p} \Big|_{h,k}^n \right) p_k^n + 2 \frac{\partial \rho}{\partial h} \Big|_{p,k}^n \left[A_j \left(\frac{T_{k+1}^n - T_k^n}{\frac{l_{k+1}}{(K_f)_{k+1}} + \frac{l_k}{(K_f)_k}} \right) - A_{j-1} \left(\frac{T_k^n - T_{k-1}^n}{\frac{l_k}{(K_f)_k} + \frac{l_{k-1}}{(K_f)_{k-1}}} \right) \right] \quad (19)$$

The enthalpies at cell junctions required for evaluation of $\Gamma_{j,k}^n$ and $\Gamma_{j-1,k}^n$ are expressed in terms of cell enthalpies using first order upwind scheme. It is not possible to simulate the dynamic behaviour of experimental facility shown in figure 1 for horizontal heater configuration from rest state using the numerical model described above. This is because of the inability of the classical 1-D models to account for natural convection. To start with, the loop is filled with water and the fluid is motionless and isothermal everywhere inside the loop. At time $t=0$, the heater power is raised from zero to some known value. Fluid inside the heater gets heated up and, with the progress of time, this hot fluid starts spreading to nearby unheated space by conduction and natural convection. Since the fluid inside the heated pipe section is warmer than that in the adjacent section on both sides, a bulk density difference is established between the two sections. The mismatch between the hydrostatic pressure fields existing on the two sides of the vertical plane separating colder and warmer sections leads to generation of convection currents between two parts. In the upper half of the pipe, the hot fluid from the warmer section starts creeping into the colder section and in the bottom half, cold fluid will creep into the heated section. It is worth mentioning that closed loop natural circulation flow rate remains zero till the hot fluid reaches either of the two vertical limbs. During the phase of natural convection, area averaged net flow at any cross section remains zero and there is a net heat transfer at the interface between hot and cold sections. The rate of heat transfer across any cross-section depends upon the net forward or backward (both are equal in magnitude for an incompressible fluid) mass flow rate at that cross section and the difference in temperatures of two stream. To account for this natural convection, Naveen Kumar et al. [16] modified Eq. (13) and (19) by incorporating an additional term in the discretized energy balance equation as given below:

$$\begin{aligned} & \rho_k^n \frac{h_k^{n+1} - h_k^n}{\Delta t} + \frac{1}{A_k} \frac{W_j^{n+1} h_j^n - W_{j-1}^{n+1} h_{j-1}^n}{l_k} - \frac{h_k^n}{A_k} \left(\frac{W_j^{n+1} - W_{j-1}^{n+1}}{l_k} \right) - \frac{(p_k^{n+1} - p_k^n)}{\Delta t} = \frac{h_{i,k} P_k (T_w^{n+1} - T_f^n)}{A_k} \\ & + \frac{1}{A_k l_k} \left[A_j \left(\frac{T_{k+1}^n - T_k^n}{\frac{l_{k+1}}{(K_f)_{k+1}} + \frac{l_k}{(K_f)_k}} \right) - A_{j-1} \left(\frac{T_k^n - T_{k-1}^n}{\frac{l_k}{(K_f)_k} + \frac{l_{k-1}}{(K_f)_{k-1}}} \right) \right] + h_{nc} \Big|_j^n (T_{k+1}^n - T_k^n) - h_{nc} \Big|_{j-1}^n (T_k^n - T_{k-1}^n) \quad (20) \\ & \Theta_k^n = \frac{\partial \rho}{\partial h} \Big|_{p,k}^n h_{i,k} P_k (T_w^{n+1} - T_f^n) + 2 \frac{\partial \rho}{\partial h} \Big|_{p,k}^n \left[A_j \left(\frac{T_{k+1}^n - T_k^n}{\frac{l_{k+1}}{(K_f)_{k+1}} + \frac{l_k}{(K_f)_k}} \right) - A_{j-1} \left(\frac{T_k^n - T_{k-1}^n}{\frac{l_k}{(K_f)_k} + \frac{l_{k-1}}{(K_f)_{k-1}}} \right) \right] \\ & - \frac{A_k l_k}{\Delta t} \left(\frac{\partial \rho}{\partial h} \Big|_{p,k}^n + \rho \Big|_k^n \frac{\partial \rho}{\partial p} \Big|_{h,k}^n \right) p_k^n + \frac{\partial \rho}{\partial h} \Big|_{p,k}^n A_k h_{nc} \Big|_j^n (T_{k+1}^n - T_k^n) - \frac{\partial \rho}{\partial h} \Big|_{p,k}^n A_k h_{nc} \Big|_{j-1}^n (T_k^n - T_{k-1}^n) \quad (21) \end{aligned}$$

The last term on right hand side of Eq. (20) has been introduced to account for energy exchange of the volume 'k' with volume 'k-1' and 'k+1' because of natural convection. The justification for adopting the particular form and

method of evaluating h_{nc} is described in Naveen Kumar et al [16]. Since there is almost zero mass transfer between the two volumes, though there is a net heat exchange, the process can be thought of as a heat exchange because of some pseudo-conductivity. The existence of this pseudo-conductivity was indirectly accounted by Muscato and Xibilia [15] and Sen et al. [17] by taking an arbitrarily high value of fluid thermal conductivity which was several orders of magnitude higher than the thermodynamic conductivity of water. Naveen Kumar et al [16] provided a theoretical basis for this enhanced conductivity. The magnitude of this pseudo-conductivity, which has the dimension of heat transfer coefficient, is given by

$$h_{nc,j} = \begin{cases} 0.99 \frac{k}{D} (Ra_D)^{1/2} & \text{for horizontal cells} \\ 3.6e^{-3} \frac{k}{D} Ra_D & \text{for vertical cells} \end{cases} \quad (22)$$

The natural convection currents are essentially multi-dimensional in nature even in small diameter pipes and develop fully only in the absence of forced convection currents. For example, in a natural circulation loop, hot fluid flows from heated section to cold sections on either side of the heater in the upper half and cold fluid is drawn from the cold section to hot section in the lower half. This implies that there is a counter motion of fluid at any given pipe cross section separating two volumes having different average temperature. There is almost net zero flow at the interface. However, when the hot fluid reaches either of the two vertical legs, the global circulation set in and mixed convection regime follows. From the physics, we know that there must be a gradual transition from natural convection to mixed convection and finally to forced convection. No well defined criterion is available in literature for demarcation among natural convection, mixed convection and forced convection regimes of convective heat transfer. Naveen Kumar et al [16] derived a criterion based on relative strength of natural convection currents and forced convection currents. The same criterion has been used in the present study also. The criterion is:

$$h_{nc} = \begin{cases} \left(1 - \frac{|u_j|}{|u_{nc,j}|}\right) h_{nc} & \text{if } |u_j| \leq |u_{nc,j}| \\ 0 & \text{if } |u_j| > |u_{nc,j}| \end{cases} \quad (23)$$

Heater Model

To simulate the heater wall dynamics, a lumped parameter model was used. The governing energy balance equation for heater is written as:

$$\rho_w A_w C_w \frac{\partial}{\partial t} (T_w) = \frac{\partial}{\partial s} \left(K_w A_w \frac{\partial T_w}{\partial s} \right) + q'' A_w + h_i P_i (T_{f,i} - T_w) - h_o P_o (T_w - T_{f,o}) \quad (24)$$

For the solution of heater energy balance equation by numerical technique, the heater is axially subdivided into the same number of control volumes as the fluid. The heater energy balance equation i.e. Eq. (24) is integrated for the control volume 'k' as shown below:

$$\begin{aligned} & -\frac{K_w \Delta t}{(\rho_w A_w C_w)_k} \frac{2A_{w,j-1}}{l_k + l_{k-1}} T_{w,k-1}^{n+1} + \left(1 + \frac{K_w \Delta t}{(\rho_w A_w C_w)_k} \left(\frac{2A_{w,j}}{l_k + l_{k+1}} + \frac{2A_{w,j-1}}{l_k + l_{k-1}} \right) + \lambda_{i,k} \Delta t + \lambda_{o,k} \Delta t \right) T_{w,k}^{n+1} \\ & - \frac{K_w \Delta t}{(\rho_w A_w C_w)_k} \frac{2A_{w,j}}{l_k + l_{k+1}} T_{w,k+1}^{n+1} = T_{w,k}^n + \frac{q'' \Delta t}{(\rho_w C_w)_k} + \lambda_{i,k} \Delta t T_{f,k}^n + \lambda_{o,k} \Delta t T_{o,k}^n \end{aligned} \quad (25)$$

$$\text{where } \lambda_{i,k} = \frac{h_{i,k} P_{i,k}}{(\rho_w A_w C_w)_k} \quad (26)$$

$$\text{and } \lambda_{o,k} = \frac{h_{o,k} P_{o,k}}{(\rho_w A_w C_w)_k} \quad (27)$$

Expansion Tank Model

All the single-phase natural circulation loops, the author has come across, are provided with an expansion tank at the highest elevation in the loop. The tank serves the twin purposes of venting air out during the loop filling and accommodation of swell and shrinkage during the transient. To the author's knowledge, no studies are available in literature on the role of expansion tank in single-phase natural circulation loop dynamics, except the one by Misale et al. [2]. In most of the numerical simulations involving use of simple tools, expansion tank is not simulated. However, most of the researchers simulating natural circulation loops consider expansion tank as a volume at constant pressure and temperature connected to main loop through a surge line. In their numerical simulation of single-phase natural circulation loops using computer code, ATHLET, Vijayan et al. [1] modelled expansion tank using a surge line and tank. Ambrosini et al. [3] and Pilkhwal et al. [4] modelled expansion tank as a time dependant volume. In order to realize the expansion tank, Misale et al. [2] connected the tank and the primary loop with two pipes. Apparently, this was done to allow some natural circulation between the tank and the main loop. Moreover, unlike the tank in actual experimental facility, it was connected in the vertical leg with two pipes connected at different elevations. However, no details of the pipe sizes, their lengths and elevation difference between the two pipes were reported. Misale et al. [2] rightly recognized that expansion tank not only keeps the loop pressure constant, it also exchanges energy with the main loop. However, the trick used by Misale et al. [2] provides neither any satisfactory explanation for energy exchange between the main loop and the expansion tank nor any workable model for simulating expansion tank. The elevation at which two pipes need to be connected and their sizes leaves much scope for subjective interpretation. In the present study, a lumped parameter model is applied for expansion tank. The model is based on following simplifying assumptions:

1. There is complete mixing of fluid in the expansion tank i.e. the temperature variation within the expansion tank is neglected.
2. The expansion tank is completely insulated. The heat loss from the expansion tank is assumed to be negligible.
3. The pressure at free surface in the expansion tank is assumed to be atmospheric.
4. The expansion tank wall heat capacity is neglected.
5. Since the velocities in the expansion tank line are small, the inertia term, friction term and acceleration terms are neglected in the momentum balance equation.
6. It is assumed that air in the expansion tank is saturated. Hence, as the temperature of liquid in the tank increases, there is evaporation of water into the air. The evaporation is assumed to be instantaneous.

With above simplifying assumptions, the governing equations for the liquid in expansion tank can be written as

Mass conservation equation

$$\frac{dm_{TK}}{dt} = W_m^{n+1} - W_0^{n+1} - \dot{m}_{vap} \quad (28)$$

Energy conservation equation

$$A_{TK} L_{TK} \frac{d}{dt}(\rho h) = \begin{cases} (W_m^{n+1} - W_0^{n+1})h_m^{n+1} - \dot{m}_{vap}(h_g - h_f) - hA_{TK}(T_f - T_{air}) & \text{if } W_m^{n+1} > W_0^{n+1} > 0 \\ -(W_m^{n+1} - W_0^{n+1})h_{TK}^{n+1} - \dot{m}_{vap}(h_g - h_f) - hA_{TK}(T_f - T_{air}) & \text{if } W_0^{n+1} > W_m^{n+1} > 0 \\ -(W_m^{n+1} - W_0^{n+1})h_0^{n+1} - \dot{m}_{vap}(h_g - h_f) - hA_{TK}(T_f - T_{air}) & \text{if } W_0^{n+1} < W_m^{n+1} < 0 \\ -(W_m^{n+1} - W_0^{n+1})h_{TK}^{n+1} - \dot{m}_{vap}(h_g - h_f) - hA_{TK}(T_f - T_{air}) & \text{if } W_m^{n+1} < W_0^{n+1} < 0 \\ -W_0^{n+1}h_0^{n+1} - W_m^{n+1}h_m^{n+1} - \dot{m}_{vap}(h_g - h_f) - hA_{TK}(T_f - T_{air}) & \text{if } W_0^{n+1} > 0; W_m^{n+1} < 0 \\ W_0^{n+1}h_0^{n+1} + W_m^{n+1}h_m^{n+1} - \dot{m}_{vap}(h_g - h_f) - hA_{TK}(T_f - T_{air}) & \text{if } W_0^{n+1} < 0; W_m^{n+1} > 0 \end{cases} \quad (29)$$

The first term on the right hand side of Eq. (29) represent the energy exchange with the loop because of swell or shrinkage in volume of liquid contained in the loop, the second term represents energy loss because of evaporation from the expansion tank and the last term represents convective heat losses.

Momentum conservation equation

$$A \frac{dp}{ds} = -\rho Ag \quad (30)$$

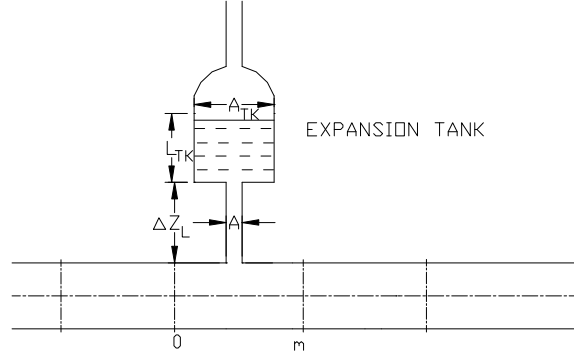


Fig. 3 Typical expansion tank connected to upper pipe of a natural circulation loop

Eq. (28) – (30) are discretized as

$$m_{TK}^{n+1} = m_{TK}^n + \Delta t (W_m^{n+1} - W_m^{n+1}) \quad (31)$$

$$A_{TK} L_{TK} \frac{(\rho_{TK}^{n+1} h_{TK}^{n+1} - \rho_{TK}^n h_{TK}^n)}{\Delta t} = \begin{cases} (W_m^{n+1} - W_0^{n+1}) h_m^{n+1} - \dot{m}_{vap} (h_g - h_f) - h A_{TK} (T_f - T_{air}) & \text{if } W_m^{n+1} > W_0^{n+1} > 0 \\ -(W_m^{n+1} - W_0^{n+1}) h_{TK}^{n+1} - \dot{m}_{vap} (h_g - h_f) - h A_{TK} (T_f - T_{air}) & \text{if } W_0^{n+1} > W_m^{n+1} > 0 \\ -(W_m^{n+1} - W_0^{n+1}) h_0^{n+1} - \dot{m}_{vap} (h_g - h_f) - h A_{TK} (T_f - T_{air}) & \text{if } W_0^{n+1} < W_m^{n+1} < 0 \\ -(W_m^{n+1} - W_0^{n+1}) h_{TK}^{n+1} - \dot{m}_{vap} (h_g - h_f) - h A_{TK} (T_f - T_{air}) & \text{if } W_m^{n+1} < W_0^{n+1} < 0 \\ -W_0^{n+1} h_0^{n+1} - W_m^{n+1} h_m^{n+1} - \dot{m}_{vap} (h_g - h_f) - h A_{TK} (T_f - T_{air}) & \text{if } W_0^{n+1} > 0; W_m^{n+1} < 0 \\ W_0^{n+1} h_0^{n+1} + W_m^{n+1} h_m^{n+1} - \dot{m}_{vap} (h_g - h_f) - h A_{TK} (T_f - T_{air}) & \text{if } W_0^{n+1} < 0; W_m^{n+1} > 0 \end{cases} \quad (32)$$

In the absence of any flow through the pipe, there will be circulation of fluid between the pipe and the expansion tank if fluid temperature in the pipe is higher than that in the tank. This fluid circulation is caused by the natural convection currents and is known as natural convection heat transfer. Naveen Kumar et al. (2011) have shown the existence of such currents both based upon scale analysis and based on CFD simulations of natural convection in a vertical cavity. The strength of natural convection flow between the pipe and the tank:

$$v_s = 3.6e^{-3} \frac{\alpha}{D} Ra_D \quad (33)$$

Under pure natural convection conditions, these currents are responsible for net heat exchange between the pipe and the expansion tank, the magnitude of which is given by

$$q'' = 3.6e^{-3} \rho c_p v_c \Delta T = 3.6e^{-3} \frac{k}{D} Ra_D \Delta T = 3.6e^{-3} \frac{k}{D} \left(\frac{g \beta D^3 ((T_o^n - T_{TK}^n))}{\nu \alpha} \right) (T_o^n - T_{TK}^n) \quad (34)$$

Since there is almost zero mass transfer between the pipe and the tank, though there is a net heat exchange, the process can be thought of as a heat exchange because of some pseudo-conductivity. The magnitude of this pseudo-conductivity, which has the dimensions of heat transfer coefficient, is given by

$$h_{nc} \Big|_{\text{exp}}^n = 3.6e^{-3} \frac{k}{D} Ra_D = 3.6e^{-3} \frac{k}{D} \left(\frac{g \beta D^3}{\nu \alpha} \right) (T_0^n - T_{TK}^n) \quad (35)$$

To account for heat exchange because of natural convection, the Eq. (32) is modified by incorporating this pseudo-conductivity term

$$A_{TK} L_{TK} \frac{(\rho_{TK}^{n+1} h_{TK}^{n+1} - \rho_{TK}^n h_{TK}^n)}{\Delta t} = \begin{cases} (W_m^{n+1} - W_0^{n+1}) h_m^{n+1} - \dot{m}_{\text{vap}} (h_g - h_f) - h A_{TK} (T_f - T_{\text{air}}) + A h_{nc} \Big|_{\text{exp}}^n (T_0^n - T_{TK}^n) & \text{if } W_m^{n+1} > W_0^{n+1} > 0 \\ -(W_m^{n+1} - W_0^{n+1}) h_{TK}^{n+1} - \dot{m}_{\text{vap}} (h_g - h_f) - h A_{TK} (T_f - T_{\text{air}}) + A h_{nc} \Big|_{\text{exp}}^n (T_0^n - T_{TK}^n) & \text{if } W_0^{n+1} > W_m^{n+1} > 0 \\ -(W_m^{n+1} - W_0^{n+1}) h_0^{n+1} - \dot{m}_{\text{vap}} (h_g - h_f) - h A_{TK} (T_f - T_{\text{air}}) + A h_{nc} \Big|_{\text{exp}}^n (T_0^n - T_{TK}^n) & \text{if } W_0^{n+1} < W_m^{n+1} < 0 \\ -(W_m^{n+1} - W_0^{n+1}) h_{TK}^{n+1} - \dot{m}_{\text{vap}} (h_g - h_f) - h A_{TK} (T_f - T_{\text{air}}) + A h_{nc} \Big|_{\text{exp}}^n (T_0^n - T_{TK}^n) & \text{if } W_m^{n+1} < W_0^{n+1} < 0 \\ -W_0^{n+1} h_0^{n+1} - W_m^{n+1} h_m^{n+1} - \dot{m}_{\text{vap}} (h_g - h_f) - h A_{TK} (T_f - T_{\text{air}}) + A h_{nc} \Big|_{\text{exp}}^n (T_0^n - T_{TK}^n) & \text{if } W_0^{n+1} > 0; W_m^{n+1} < 0 \\ W_0^{n+1} h_0^{n+1} + W_m^{n+1} h_m^{n+1} - \dot{m}_{\text{vap}} (h_g - h_f) - h A_{TK} (T_f - T_{\text{air}}) + A h_{nc} \Big|_{\text{exp}}^n (T_0^n - T_{TK}^n) & \text{if } W_0^{n+1} < 0; W_m^{n+1} > 0 \end{cases} \quad (36)$$

$$(p_{\text{atm}} - p_0^{n+1}) = -\rho_{m,s}^n (L_{TK}^{n+1} + \Delta Z_L) g \quad (37)$$

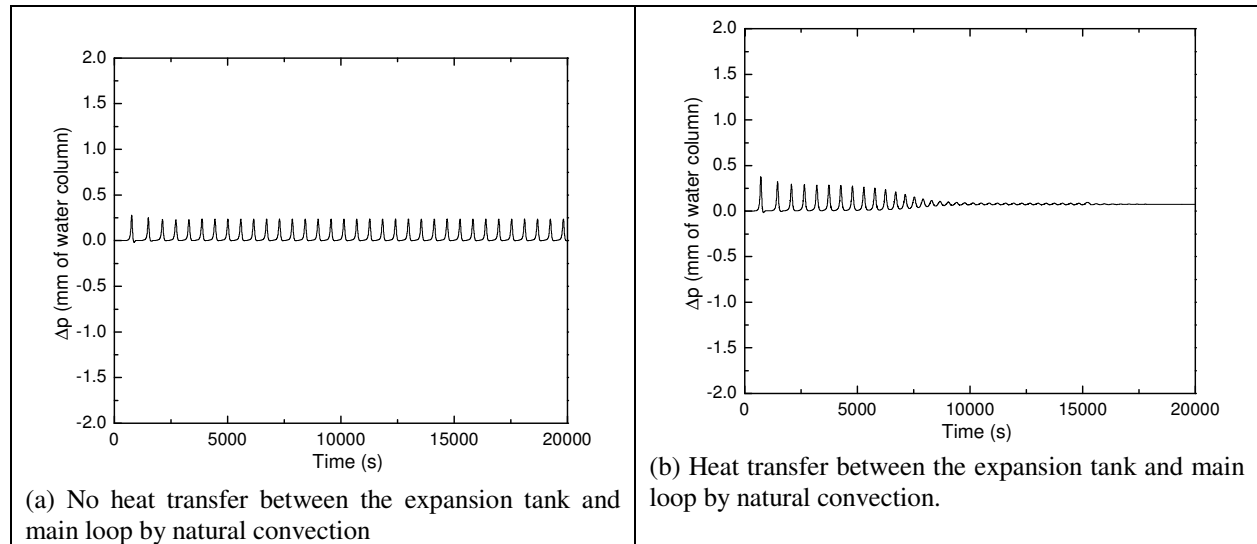


Fig.4: Prediction of transient behaviour obtained by the model developed for a heater power input of 25W.

RESULTS AND DISCUSSIONS

Experimental investigations by Misale et al. [2] show that temperature in the expansion tank is not constant during the test. This leads to a delay in the primary natural circulation loop temperature rise. However, no experimental data was presented regarding the initial level in expansion tank and the rate of temperature rise. To the best of the authors' knowledge, in none of the experimental results reported, there is no data about the status of expansion tank. In the results reported in [10, 11], the expansion tank temperature and level were not recorded. In absence of information about initial temperature and initial level of water in the expansion tank, it is not possible to evaluate the evaporation and convective heat losses from expansion tank water in Eq. (36). The authors could have used some arbitrary value for the initial fluid level and temperature in the loop. However, that could have been

equivalent to fine tuning of parameters to match the numerical simulations with the experimental data. Under stable steady state operating conditions, these terms help in stabilizing the expansion tank temperature at some steady state value for a given heater power. Under steady state operation, the rate of heat transport from main loop to the tank by pseudo-conduction (last term in Eq. (36)) is balanced by the evaporation losses and convection heat losses from the tank liquid. Therefore, dropping of evaporation loss and convective heat transfer terms from Eq. (36) poses additional problems to numerical simulations.

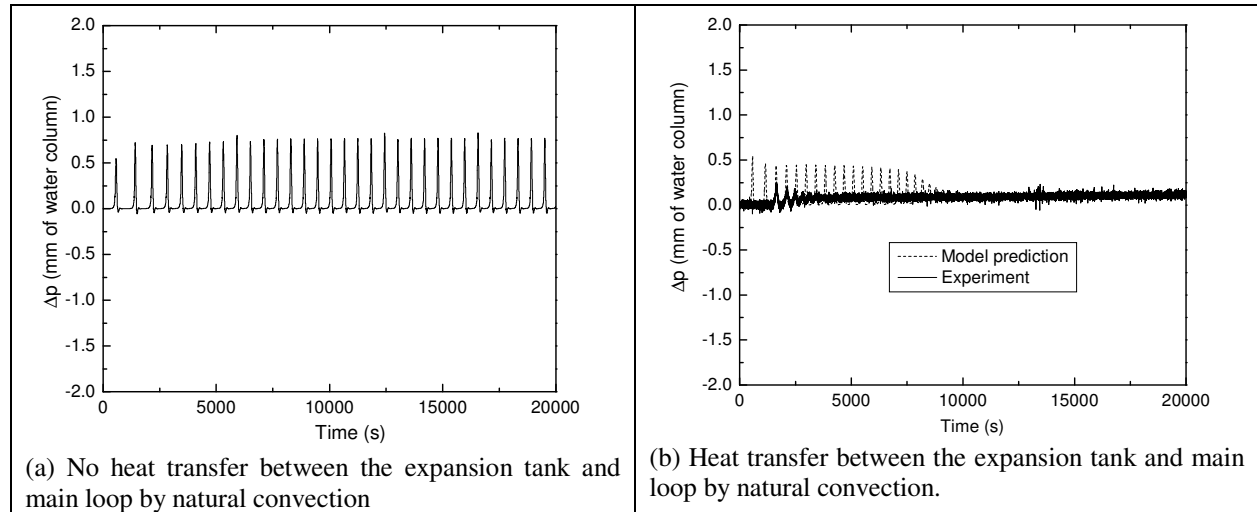


Fig.5: Prediction of transient behaviour obtained by the model developed for a heater power input of 45W.

The purpose of the present study is to bring out the role of expansion tank in single-phase loop dynamics and phenomena of hysteresis observed in these loops. Therefore, authors have dropped the evaporation loss and convective heat transfer terms from Eq. (36). This is a valid assumption for simulations at low powers for which the results are presented. The expansion tanks have large volumes and at low power the rise in temperature is expected to be very small. Hence, to bring out the physics, the authors have carried out two types of numerical simulations, one without any heat exchange between the expansion tank and one with heat exchange between the expansion tank and the main loop by natural convection. Figure 4 shows the model predictions for a heater power input of 25W for start up from rest state for two different cases: (a) no heat transfer between the expansion tank and main loop by natural convection; (b) heat transfer between the expansion tank and main loop by natural convection. From figure 4, it is clear that the loop stability characteristics cannot be predicted correctly even for a very low power also without considering the expansion tank. In fact, in numerical simulations without expansion tank model, the start up from rest always predicts unstable behaviour irrespective of the heater power input. Figure 5 shows the model predictions for a heater power input of 45W for start up from rest state for two different cases: (a) no heat transfer between the expansion tank and main loop by natural convection; (b) heat transfer between the expansion tank and main loop by natural convection. From figure 5(b), it is clear that the pressure drop across the heater predicted by the model matches closely with the experimental data. However, the amplitude of initial oscillations predicted by the model is higher than that observed in the experiments. This can be attributed to the heater model adopted in the present study. The experimental facility consists of a heater made up of 1 mm diameter nichrome wire evenly wound on the outside of the glass tube. In this type of the heaters, all the heat generated does not go to the wall immediately. During the initial part, a part of the heater power input goes to the insulation as well. However, in the model adopted for heater wall dynamics, it is assumed that all the power goes to tube wall.

For higher powers, the loop behaviour cannot be predicted accurately without considering the evaporation and convective heat losses from expansion tank fluid. However, at this stage some important inferences can be drawn about the role of expansion tank in the phenomena of hysteresis observed in the experimental facility. During start-up from rest, the temperature in the fluid temperature in the expansion tank is same as that of the fluid in the main loop. Therefore, during power raising from rest, the expansion tank acts as a additional heat sink. This has a stabilizing effect on loop dynamics. However, when the loop is started at a power higher than the lower threshold (greater than 105 W in the present case), the fluid temperature in the expansion tank increases and subsequently

when the power is decreased, this heat sink is not available because the fluid temperature is higher. Hence, loop stabilizes at a power lower than that obtained when power is raised.

CONCLUSIONS

This work clearly brings out the role of expansion tank in single-phase natural circulation loop dynamics. A lumped parameter model has been presented for predicting the expansion tank behaviour. The model has been successfully integrated with a 1-D model developed previously. Expansion tank model helps in predicting the lower stability threshold of instability as observed in experimental investigations. The energy exchange between the expansion tank and the main loop has a stabilizing effect. The phenomena of hysteresis observed in experimental investigations on single-phase natural circulation loops by Vijayan et al. [11] is mainly because of the expansion tank. A possible explanation for the same has been inferred from the model predictions. The simple single-phase natural circulation loops have been used over the years for fundamental studies related to development of new models and improvement in existing models and for understanding the physics of unstable behaviour. The results presented in this paper helps in underlying the importance of like expansion tank in loop instability.

Natural circulation systems have been used in existing nuclear power plants like VK-50 and Dodewaard reactors for core heat removal under normal operating conditions. Many of the next generation nuclear power plants like AHWR, ESBWR and CAREM propose to use natural circulation for core heat removal during normal as well as off-normal conditions while many other next generation nuclear power plants like AP-600, AP-1000, VVER-1000, HTGR and GFR propose to use natural circulation for core decay heat removal. However, it is a well known fact that natural circulation systems have low driving force and there is an urgent need to assess the reliability and performance of natural circulation systems before they can be fully relied for core heat removal. Since the existing system codes are unable to take into account the complex behaviour exhibited by natural circulation systems under low flow conditions, there is urgent need to reassess and improve the capabilities of system codes for application to natural circulation systems.

NOMENCLATURE

A	area of Cross Section, m ²		Greek Symbols
C, C _p	specific heat at constant pressure, kJ/kg.K	α	thermal diffusivity, m ² /s
D	pipe diameter, m	β	coefficient of thermal expansion, K ⁻¹
D _h	hydraulic diameter, m	θ	angle subtended by the pipe with vertical, radian
F	Darcy's friction factor	μ	fluid viscosity, Pa.s
G	gravitational acceleration, m/s ²	ν	kinematic viscosity, m ² /s
H	specific enthalpy (kJ/kg), heat transfer coefficient (W/m ²)	ρ	density, kg/m ³
h _{nc}	pseudo-conductivity per unit area, W/ m ² .K		
K	thermal conductivity, W/m.K		Subscripts
L	cell length, m	f	fluid
M	mass, kg	g	vapour
P	pressure, Pa	i	inner
P	perimeter, m	j	junction index
Pr	Prandtl number, C _p μ /K	k	cell index
q'''	volumetric heat generation rate, W/m ³	nc	natural convection
Ra _D	Rayleigh number, (D ³ $\rho^2\beta g\Delta T/\nu\alpha$)	o	outer
S	running coordinate, m	TK	tank
T	time, s	vap	vaporization
u,v	fluid velocity, m/s		
W	mass flow rate, kg/s		
Z	elevation, m		

REFERENCES

- [1] Vijayan, P.K., Austregesilo, H., Teschendorff, V., "Simulation of the unstable oscillatory behavior of single-phase natural circulation with repetitive flow reversals in a rectangular loop using the computer code ATHLET", Nucl. Eng. Des., Vol. 155, 1995, pp. 623-641.
- [2] Misale, M., Frogheri, M., D'Auria, F., Fontani, E., Garcia, A., "Analysis of single-phase natural circulation experiments by system codes", Int. J. Ther Sci, Vol. 38, 1999, pp. 977-983.
- [3] Ambrosini, W., Forgione, N., Ferreri, J.C., Bucci, M., "The effect of wall friction in single-phase natural circulation stability at the transition between laminar and turbulent flow", Ann. Nucl. Energy, Vol. 31, 2004, pp. 1833-1865.
- [4] Pilkhwal D.S., Ambrosini W., Forgione N., Vijayan P.K., Saha D., Ferrari J. C., " Analysis of the unstable behaviour of a single phase natural circulation loop with one dimensional and computational fluid dynamics models" Ann. Nucl. Energy, Vol. 34, 2007, pp. 339-355.
- [5] Bau, H.H., Torrance, K.E., "Transient and steady behavior of an open symmetrically heated, free convection loop", Int. J. Heat Mass Transfer, Vol. 24, 1981, pp. 597-609.
- [6] Zvirin, Y., "A review of natural circulation loops in pressurized water reactors and other systems", Nucl. Eng. Des., Vol. 67, 1981, pp. 203-225.
- [7] Chen K., "On the oscillatory instability of closed loop thermosyphons", J. Heat Transfer, Trans. ASME, Vol. 107, 1985, pp. 826-831.
- [8] Gordon, M., Ramos, E., Sen, M., "One dimensional model of a thermosyphon with known wall temperature" Int. J. Heat Fluid Flow, Vol. 8, 1987, pp. 177-181.
- [9] Vijayan, P.K., Austregesilo, H., "Scaling laws for single-phase natural circulation loops", Nucl. Eng. Des., Vol. 152, 1994, pp. 331-347.
- [10] Vijayan, P.K., Bhojwani, V.K., Bade, M.H., Sharma, M., Nayak, A.K., Saha, D., Sinha, R.K., "Investigations on the effect of heater and cooler orientation on the steady state, transient and stability behaviour of single-phase natural circulation in a rectangular loop", Bhabha Atomic Research Centre, Report BARC/2001/E/034.
- [11] Vijayan, P.K., Sharma, M., Saha, D., "Steady state and stability characteristics of single-phase natural circulation in a rectangular loop with different heater and cooler orientations" Exp. Therm. Fluid Sci., Vol. 31, 2007, pp.925-945.
- [12] Ambrosini, W., Ferreri, J.C., "The effect of truncation error on numerical prediction of stability boundaries in a natural circulation single phase loop", Nucl. Eng. Des., Vol. 183, 1998, pp. 53-76.
- [13] Ambrosini, W., Ferreri, J.C., "Stability analysis of single phase thermosyphon loops by finite difference numerical methods", Nucl. Eng. Des., Vol. 201, 2000, pp. 11-23.
- [14] Ambrosini, W., Ferreri, J.C., "Prediction of stability of one-dimensional natural circulation with a low diffusion numerical scheme", Ann. Nucl. Energy, Vol. 30 (15), 2003, pp. 1505-1537.
- [15] Muscato, G., Xibilia, M.G., "Modeling and control of a natural circulation loops. J. Process. Control, Vol. 13, 2003, pp. 239-251.
- [16] Naveen Kumar, Doshi, J.B., Vijayan, P.K., "Investigations on the role of mixed convection and wall friction factor in single-phase natural circulation loop dynamics", Annals of Nuclear Energy, Vol. 38(10), 2011, pp. 2247-2270.
- [17] Sen, M., Pruzan, D. A., and Torrance, K. E., "Analytical and experimental study of steady state convection in a double loop thermosyphon", Int. J. Heat Mass Transfer, Vol. 31, 1988, 709-722.